

Cellular Automata Automatically Constructed from a Bioconvection Pattern

Akane Kawaharada, Erika Shoji, Hiraku Nishimori, Akinori Awazu,
Shunsuke Izumi and Makoto Iima

Abstract We construct cellular automaton models for the spatio-temporal pattern of *Euglena gracilis* bioconvection, which is generated when a suspension of *Euglena gracilis* is illuminated from the bottom with strong light intensity through a statistical construction method of cellular automata. The method of construction is introduced by Kawaharada and Iima (A. Kawaharada and M. Iima, “Constructing Cellular Automaton Models from Observation Data”, In 2013 First International Symposium on Computing and Networking, pp. 559–562 (2013)). Some features of the original patterns are reproduced by one dimensional deterministic CA with the nearest three neighbors and eight possible states for a site.

Keywords *Euglena gracilis* · Bioconvection · Spatio-temporal pattern · Cellular automata · Observation data · Constructing method of cellular automata

1 Introduction

Collective behavior of animals from microorganisms to birds, form various patterns, e.g. formation flight of geese, bait ball of sardine, bacterial colonies, and bioconvections. Such patterns are generated by hierarchical mechanisms including self-propelling of individuals, hydrodynamic, mechanic, or chemical interactions among individuals, and effects from the surrounding environment generated through their macroscopic behavior.

A. Kawaharada (✉) · E. Shoji · H. Nishimori · A. Awazu · S. Izumi · M. Iima
Hiroshima University, 1-3-1 Kagamiyama, Higashi-Hiroshima 739-8526, Japan
e-mail: a-kwprd@u-shizuoka-ken.ac.jp

A. Kawaharada · M. Iima
Core Research for Evolutional Science and Technology, Japan Science
and Technology Agency, 5, Sanbancho, Tokyo, Chiyoda-ku 102-0075, Japan

H. Nishimori · A. Awazu
Research Center for the Mathematics on Chromatin Live Dynamics,
Hiroshima-University, 1-3-1 Kagamiyama, Higashi-Hiroshima 739-8530, Japan

In this study, we focus on the ordered patterns generated in bioconvection, a collective behavior of microorganisms in fluid caused by their behavioral responses of individuals to stimuli (*taxes*) (Pedley and Kessler 1992; Hill and Pedley 2005). The microorganism used in the experiment is *Euglena gracilis*, a unicellular flagellate whose body length is approximately $50 \sim 100 \mu\text{m}$ long. *E. gracilis* has phototaxis; it escapes from light sources with strong light intensity (over 200 W/m^2 ; negative phototaxis) and approaches light sources with weak light intensity (below 200 W/m^2 ; positive phototaxis). If a suspension of *E. gracilis* is illuminated from the bottom with strong light intensity, the individuals accumulate near the surface because of negative phototaxis. Because the density of *E. gracilis* is heavier than water, parts of the *Euglena*-rich regions fall down to drive the local flow. Such interaction between the individuals and the flow eventually forms bioconvection patterns. Their bioconvection patterns are peculiar because they can form spatially localized patterns (Suematsu et al. 2011) which have been experimentally simplified to extract fundamental patterns (Shoji et al. 2014) similar to those observed in binary fluid convection (Watanabe et al. 2012). However, we focus on branch-like spatio-temporal patterns of the bioconvection covering the whole region, which is observed when the number density is relatively large in the case of Refs. (Suematsu et al. 2011; Shoji et al. 2014).

Because the governing equation of the bioconvection of *E. gracilis* is not determined although hydrodynamic models incorporating lateral phototaxis have been proposed (Iima et al. 2014), we need an alternative way to understand their pattern formation mechanism. In some cases, constitutive models are constructed by assuming the interaction functions. Such modeling method can be applied to wide range of phenomena, however, created models are not unique in general and has fitting parameters. As a result, such models are difficult to give qualitative prediction.

In this paper, we will choose another approach to construct the model by utilizing cellular automaton (CA), a discrete dynamical system in which the time evolution of the configuration is determined by local rules acting on each site in synchronous. Compared with various formulations of the target models, CA has the following two advantages. The first advantage is that CA has both mathematical simplicity and the potential to describe complex phenomena even from simple rules. Because CA can be mathematically regarded as an extension of symbolic dynamics (Bruce Kitchens 1998; Lind and Marcus 1995) and \mathbb{Z}^D -action, which is the ergodic theory on D -dimensional lattice (Keller 1998), the dynamics of CAs have been studied well (e.g., Hedlund 1969; Kurka 2001; Hurley 1990; Milnor 1988; Meyerovitch 2008; Kawaharada 2013). Also, CAs have been used as mathematical models of various phenomena, e.g., fluid dynamics (Hardy et al. 1973, 1976; Frisch et al. 1986; McNamara and Zanetti 1988), chemical reactions (Gerhardt et al. 1990; Gerhardt 1990), pattern formations of living matters (Kusch and Markus 1996; David Young 1984).

The second advantage is that we can construct CA through data of a phenomenon without any interpretations; this method has been recently proposed by Kawaharada and Iima (Kawaharada and Iima 2013). In this method, CA models are constructed not by intuition but by statistical analysis, thus, we do not need to assume interaction functions to construct a CA model. We assume that the target phenomenon is

determined by local governing rules that is homogeneous in space and time. After discretizing the data and assuming the interaction range, we can obtain their propagating rules through statistical analysis of the observation data.

This method has been applied to the data generated by the diffusion equation and the Burgers equation (Kawaharada and Iima 2014), and it has been shown that at least qualitative behavior of the equations can be reproduced by stochastic CAs. However, this method has never been applied to real-life phenomena, i.e., observed data in nature.

In this paper, we have applied this CA construction method to the observation data of spatio-temporal patterns in *E. gracilis* bioconvection. We show that the obtained CA reproduces features of the bioconvection patterns. This paper is organized as follows. In Sect. 2 we give the results of the experiment. In Sect. 3 we construct CAs from the data of *E. gracilis*. Finally, Sect. 4 summarizes concluding remarks.

2 Spatio-Temporal Patterns in *E. Gracilis* Bioconvection

In this section we briefly explain the experimental set-up and the experimental results.

2.1 Experimental Set-Up

An annular container with outer radius 25 mm and inner radius 20 mm was used (Fig. 1a). Both the radial width and the suspension depth d were fixed to 5 mm. The density of *E. gracilis* suspension is 7.5×10^5 cells/mL, which was prepared by the same procedure used in (Suematsu et al. 2011). The surface of the suspension was not covered. The container was illuminated from the bottom by LED light plate whose light intensity was 1520lx. The spatio-temporal patterns of the number density were recorded by a digital video camera (JVC GC-PX1) from the side, and the line near the surface (x-axis in Fig. 1b) was used to construct the spatio-temporal pattern. The experiment was performed for 15000 s long to record the pattern formation process.

2.2 Spatio-Temporal Pattern

Typical dynamics among *Euglena*-rich regions consist of the creation, the merge, and interactions between the *Euglena*-rich regions. The creation process is shown by a series of pictures taken from the side in Fig. 2a. In the red circle drawn in the top of the picture, a *E. gracilis*-rich region is being created, which is indicated by the following pictures showing that the *E. gracilis*-rich region is falling down. The merging process is shown in Fig. 2b. In the red circle drawn in the top picture, two bright regions are shown. In both regions, *Euglena* falls down. A series of pictures show that the right region becomes weaker and eventually it is absorbed in left region.

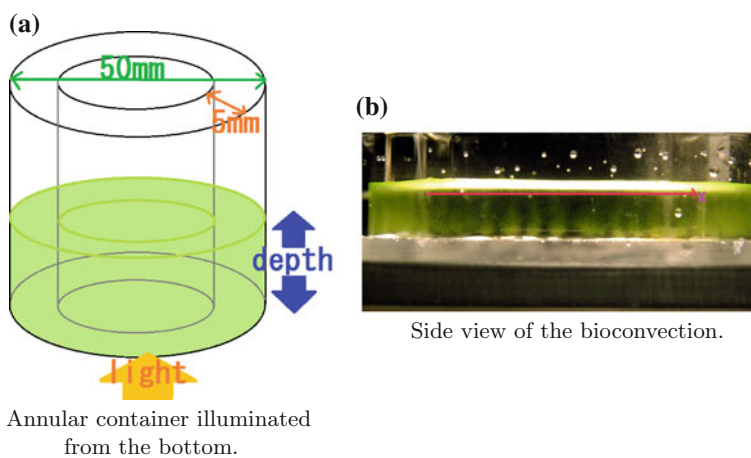


Fig. 1 Annular container used in the experiment

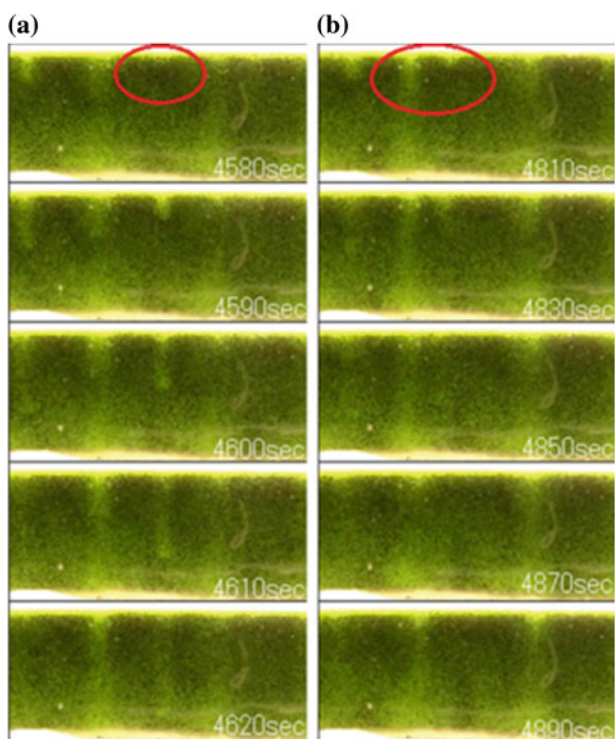
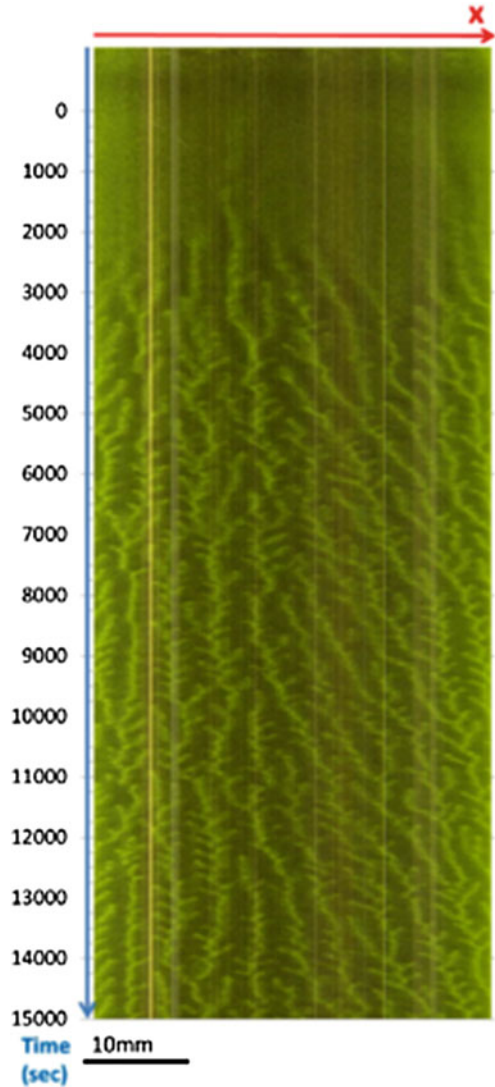


Fig. 2 **a** Sequence of creation process of a *Euglena*-rich region (4580–4630s). **b** Sequence of merge process of two *Euglena*-rich regions (4810–4890s)

Fig. 3 Spatio-temporal patterns
 ($\rho = 7.5 \times 10^5$ cells/ml)



Although the elementary processes can be explained as the creation and the merge of the *E. gracilis*-rich regions, the total dynamics can be understood only by the global spatio-temporal patterns. In Fig. 3, the spatio-temporal pattern of the bioconvection was shown. The horizontal axis corresponds to the line of Fig. 1b and the vertical line corresponds to time evolution. Bright green parts show *E. gracilis*-rich regions in which individuals of *E. gracilis* fall down (see also the side view in Fig. 1b). The pattern shows up until about 2000s, near which the *E. gracilis*-rich regions emerge. The *E. gracilis*-rich regions are not stationary; they move leftward or rightward due

to the interaction among other *E. gracilis*-rich regions through generated flow and/or the number density wave of *E. gracilis*, although the details have not been fully understood. The pattern looks like trees; small branches stem from main branches. Because time evolves from top to down, the bright region representing branch actually created, then it merges to another bright region representing another branch. The motion of thick (brighter) regions can not be explained by the elementary process of the local bright region, and another approach should be considered. In the next section, we will show an alternative approach, construction of CA.

3 Constructing Cellular Automata from Data of *E. Gracilis*

In this section we introduce the statistical method of constructing CA models from the observation data introduced in (Kawaharada and Iima 2013, 2014) and apply this method to the data of the dynamics of *E. gracilis*. We also compare the patterns created by the obtained CA with the original spatio-temporal pattern in *E. gracilis* bioconvection.

3.1 The Constructing Method of CAs Directly from Observation Data

First, we present definitions on CAs. A *discrete dynamical system* is defined by (X, T) consisting of a space X and a transformation $T : X \rightarrow X$. Let $A = \{0, \dots, k-1\}$ ($k \geq 1$) be a finite *state set* and \mathbb{Z} be a set of integers. A *configuration space* is defined by $A^{\mathbb{Z}}$ and each element of $A^{\mathbb{Z}}$ is called a *configuration*. For a configuration $x \in A^{\mathbb{Z}}$ the *shift transformation* σ is defined by $(\sigma x)_l = x_{l+1}$ for each $l \in \mathbb{Z}$.

Definition 1 Let T be a shift-commuting transformation on $A^{\mathbb{Z}}$, i.e., $T \circ \sigma = \sigma \circ T$. A discrete dynamical system $(A^{\mathbb{Z}}, T)$ is a *cellular automaton* (CA), if T is given by for $x \in A^{\mathbb{Z}}$ and each coordinate $l \in \mathbb{Z}$ and $l_1, \dots, l_m \in \mathbb{Z}$

$$(Tx)_l = f(x_{l+l_1}, \dots, x_{l+l_m}), \quad (1)$$

where f is a map from A^m to A , called a *local rule*.

Next, we briefly summarize the construction method of CAs from data. The detailed procedure and applications to some partial differential equations are in (Kawaharada and Iima 2013, 2014). A CA rule needs to be defined locally, but in many cases we only observe the macroscopic spatio-temporal behavior of a phenomenon (e.g. recorded movie), even though a local rule actually governs the phenomenon. To extract the CA rule, the following procedure is proposed. First, we predetermine the number of the states of a site k , and discretize the observation data accordingly. Next, based on the predetermined the number of neighbors m , we

calculate the frequency of appearance of the states $(Tx)_l$ for each combination of possible states of neighbors $\{x_{l+l_1}, \dots, x_{l+l_m}\}$. We define local rules of CA using the frequency of appearance of the states. If we need a deterministic rule, the rule is defined by the state which gives maximum appearance of the state. Another choice is to define a stochastic rule, in which each rule is selected according to the frequency of the appearance of the state. The definition of the stochastic CA and applications are discussed in Refs. (Kawaharada and Lima 2013, 2014).

This method implies that we can extract the hidden mechanism of a phenomena even if the macroscopic behavior is much complicated, as far as the mechanism is determined locally. A demonstration of reconstruction of CA rule from noise-contaminated CAs (Rule 90 and Rule 150) are discussed in (Kawaharada and Lima 2013, 2014).

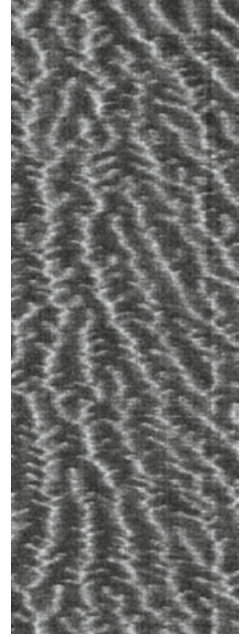
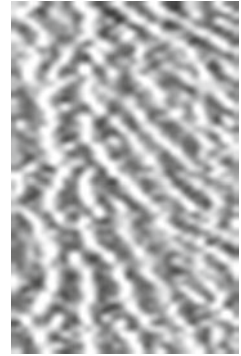
3.2 CA of the Bioconvection of *E. Gracilis* Obtained from Spatio-temporal Data

The construction method was applied to the spatio-temporal data of *E. gracilis* bioconvection (Fig. 3). Here, we report the deterministic CA for the case $k = 8, m = 3$, and $\{l_1, l_2, l_3\} = \{-1, 0, 1\}$. The detailed procedure to discretize the spatio-temporal data was as follows.

1. Figure 3 was converted to the gray scale image, then external noise (unnecessary vertical lines) was removed before the contrast was adjusted. Central part of the image was extracted (Fig. 4). The image size is $L_x \times L_t$ pixels ($L_x = 362, L_t = 3936$).
2. The filtered image (Fig. 4) was discretized by the local averaging; the average was performed in the region $[c_x N_x, c_x(N_x + 1)) \times [c_t N_t, c_t(N_t + 1))$ ($N_x = 0, 1, \dots, L'_x - 1, N_t = 0, 1, \dots, L'_t - 1$), where c_x and c_t are integer parameters which define the spacial scale and the temporal scale of interest, respectively, and $L'_x = \lfloor L_x/c_x \rfloor, L'_t = \lfloor L_t/c_t \rfloor$. The averaged value at each site, u , was discretized to give the state of CA, $a \in A = \{0, 1, \dots, 7\}$, such that $u/(u_{\max} - u_{\min}) \in [a/k, (a+1)/k)$ where u_{\max} is the max value of u and u_{\min} is the minimum in the whole data. In this paper, we show the case $c_x = 9$ and $c_t = 17$ (Fig. 5). The image size is $L'_x \times L'_t$ pixels ($L'_x = 40, L'_t = 231$). Because of the scales we chose, the major structure of the image is now straight lines or inclined lines which are white, and fine branches stemming from the major branch is not very clear.

Using the discretized data, we can define both deterministic and stochastic CA by the procedure in Sect. 3.1. In this paper, we show the results of deterministic CA, because the stochastic CA gave bleary spatio-temporal patterns which did not include the macroscopic characteristic structures.

When the observed data is not sufficiently long, some local rule can be indeterminate because no combination of $\{x_{-1}, x_0, x_1\}$ is observed under the given data, which

Fig. 4 Filtered data**Fig. 5** Discretized data with $c_x = 9, c_t = 17$ 

will be referred to as “empty rule”. Although there can be several choices to define the rule of the empty rule, we defined the rule of such cases to give the discretized state $k - 1$ for the sites. This principle gives a nucleation of *Euglena*-rich region.

The spatio-temporal pattern obtained from the constructed CA is shown in Fig. 6a. The initial configuration is given by a random number in A for each site. In this example, the straight lines and inclined lines in Fig. 5 are not perfectly reproduced. However, the patterns generated in Fig. 6a have the following properties; Straight lines are generated after initial transient (α in Fig. 6a). The patterns in the middle part arises from a complex combination of some triangle-like structures (β in Fig. 6a). We can see upward left side branches in the original pattern (γ in Fig. 6a). There are

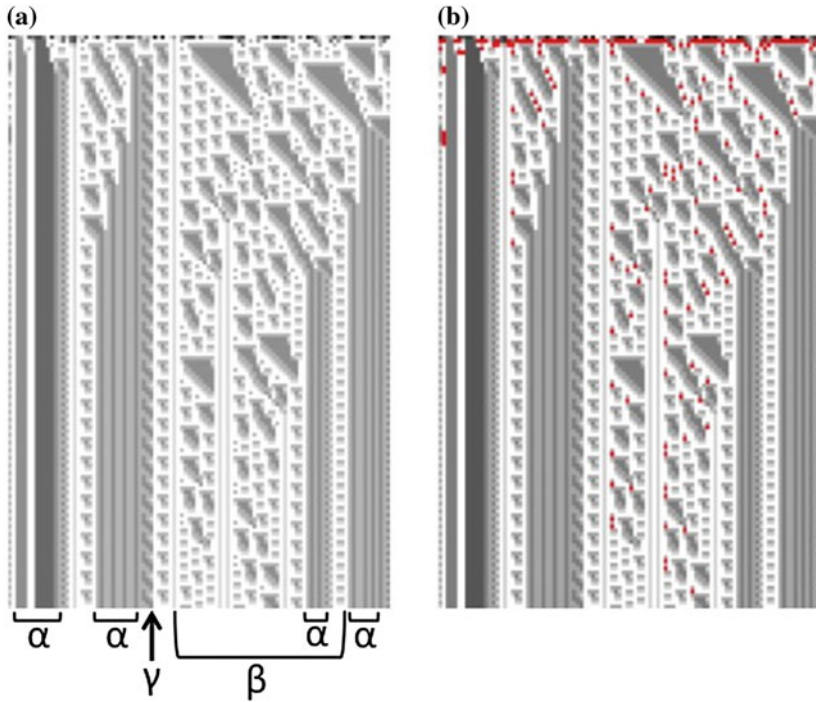


Fig. 6 Spatio-temporal patterns of the obtained CA

no right side branches because deterministic CA rule chosen here forces the pattern to grow either leftward or rightward.

The frequency that the empty rule occurs during generating the spatio-temporal pattern becomes much smaller very quickly. Actually, the number of the empty rules was 348 out of $512 (= 8^3)$ local rules in the determined CA. Thus, only $(512 - 348)/512 \simeq 32\%$ of the local rules was determined in the CA. At a glance, the ratio of the empty rules looks too large to determine the spatio-temporal pattern of the original data. However, the ratio of the empty rules becomes significantly lower after initial transient. Figure 6b is the same spatial-temporal pattern as Fig. 6a with the same initial configuration except for the red dots, the cells which was determined by the empty rule. Figure 6b clearly shows that the appearance frequency of the red dots becomes significantly lower very quickly; in fact the frequency of the empty rule becomes $125/14800 \simeq 0.8\%$ when the first two rows are removed. This result shows that the most part of the spatio-temporal pattern by the CA is determined by only about 32% or less local rules after initial transients. Further, the number of local rules necessary to reproduce typical patterns is much smaller compared with the total number of local rules. Actually, the patterns α and γ do not include any empty rules, which means that these patterns are reproduced by the rule generated

from the observation data alone. The pattern β , however, contains several red dots after initial transient. Thus, the pattern β may depend on our definition for the empty rule.

4 Concluding Remarks

In this paper, we have constructed CA models for the spatio-temporal patterns in *E. gracilis* bioconvection. Because the rules of CA are determined statistically, we need no knowledge of bioconvection; we simply discretize the data and counting the number of observed rules among all the possible rules. In this method, the modeling parameters are the time width and the spatial width to discretize the data, number of states at each site, and number of neighbors. As a result, we have many CAs from even single spatio-temporal data. Among such CAs, we can obtain some CA rules that produce patterns which share some similarities in common with the observation data.

Here we simply demonstrated that we can produce interesting patterns from the observation data. In this method, our knowledge of the phenomena is not prerequisite for the model construction. However, if we want to reproduce the features of the original phenomena, it is easy to modify the CA rule according to our knowledge of the phenomena. For example, in the case of bioconvection, generation of branch is hard to give the deterministic CA rule because a nucleation process is stochastic. If we want, it is easy to include this effect by a perturbation term. Further application of this method will be reported elsewhere.

References

- Pedley, T.J., Kessler, J.O.: Hydrodynamic phenomema in suspensions of swimming microorganisms. *Ann. Rev. Fluid Mech.* **24**, 313–358 (1992)
- Hill, N.A., Pedley, T.J.: Bioconvection. *Fluid Dyn. Res.* **37**(1–2), 1–20 (2005)
- Suematsu, N.-J., Awazu, A., Izumi, S., Noda, S., Nakata, S., Nishimori, H.: Localized bioconvection of *Euglena* caused by Phototaxis in the lateral direction. *J. Phys. Soc. Jpn.* **80**(6), 064003 (2011)
- Shoji, E., Nishimori, H., Awazu, A., Izumi, S., Iima, M.: Localized bioconvection patterns and their initial state dependency in *Euglena gracilis* suspensions in an annular container. *J. Phys. Soc. Jpn.* **83**, 043001 (2014)
- Watanabe, T., Iima, M., Nishiura, Y.: Spontaneous formation of travelling localized structures and their asymptotic behaviour in binary fluid convection. *J. Fluid Mech.* **712**, 219–243 (2012)
- Iima, M., Shoji, E., Suematsu, N., Awazu, A., Izumi, S., Nishimori, H.: A Governing Equation of Localized Bioconvection Patterns in *Euglena gracilis* Suspensions. (in preparation)
- Kitchens, B.P.: *Symbolic Dynamics: One-Sided, Two-Sided and Countable State Markov Shifts*. Universitext. Springer, Berlin (1998)
- Lind, D., Marcus, B.: *An Introduction to Symbolic Dynamics and Coding*. Cambridge University Press, Cambridge (1995)
- Keller, G.: *Equilibrium States in Ergodic Theory*. London Mathematical Society Student Texts, vol. 42. Cambridge University Press, Cambridge (1998)

- Hedlund, G.A.: Endomorphisms and automorphisms of the shift dynamical system. *Math. Syst. Theory* **3**, 320–375 (1969)
- Kurka, P.: Topological dynamics of cellular automata. In: *Codes, Systems, and Graphical Models*, Minneapolis, MN, 1999. The IMA Volumes in Mathematics and its Applications, vol. 123, pp. 447–485. Springer, New York (2001)
- Hurley, M.: Attractors in cellular automata. *Ergodic Theory Dynam. Syst.* **10**(1), 131–140 (1990)
- Milnor, J.: On the entropy geometry of cellular automata. *Complex Syst.* **2**(3), 357–385 (1988)
- Meyerovitch, T.: Finite entropy for multidimensional cellular automata. *Ergodic Theory Dynam. Syst.* **28**(4), 1243–1260 (2008)
- Kawaharada, A.: Ulam’s cellular automaton and rule 150. *Hokkaido Math. J.* (to be published)
- Hardy, J., Pomeau, Y., de Pazzis, O.: Time evolution of a two dimensional model system. i. invariant states and time correlation functions. *J Math. Phys.* **14**(12), 1746–1759 (1973)
- Hardy, J., de Pazzis, O., Pomeau, Y.: Molecular dynamics of a classical lattice gas: transport properties and time correlation functions. *Phys. Rev. A* **13**, 1949–1961 (1976)
- Frisch, U., Hasslacher, B., Pomeau, Y.: Lattice-gas automata for the Navier-Stokes equation. *Phys. Rev. Lett.* **56**, 1505–1508 (1986)
- McNamara, G., Zanetti, G.: Use of the Boltzmann equation to simulate lattice gas automata. *Phys. Rev. Lett.* **61**(20), 2332–2335 (1988)
- Gerhardt, M., Schuster, H., Tyson, J.J.: A cellular automaton model of excitable media: Ii. curvature, dispersion, rotating waves and meandering waves. *Physica D* **46**(3):392–415 (1990)
- Gerhardt, M., Schuster, H., Tyson, J.J.: A cellular automaton model of excitable media: Iii. fitting the belousov-zhabotinskii reaction. *Physica D* **46**(3):416–426 (1990)
- Kusch, I., Markus, M.: Mollusc shell pigmentation: cellular automaton simulations and evidence for undecidability. *J. Theoret. Biol.* **178**(3), 333–340 (1996)
- Young, David A.: A local activator-inhibitor model of vertebrate skin patterns. *Math. Biosci.* **72**(1), 51–58 (1984)
- Kawaharada, A., Iima, M.: Constructing cellular automaton models from observation data. In: *2013 First International Symposium on Computing and Networking*, pp. 559–562 (2013)
- Kawaharada, A., Iima, M.: An application of data-based construction method of cellular automata to physical phenomena. *J. Cell. Automata* 1–21 (2014) (submitted)

Recent Advances in Natural Computing

Selected Results from the IWNC 8 Symposium

Suzuki, Y.; Hagiya, M. (Eds.)

2016, VIII, 118 p. 69 illus., 42 illus. in color., Hardcover

ISBN: 978-4-431-55428-8